Journal of Applied Physics ARTICLE scitation.org/journal/jap

Ultrathin atomic layer deposited niobium oxide as a passivation layer in silicon based photovoltaics

Cite as: J. Appl. Phys. **130**, 215301 (2021); doi: 10.1063/5.0067281
Submitted: 15 August 2021 · Accepted: 11 November 2021 ·
Published Online: 7 December 2021

Connor J. Leach,[1] Benjamin E. Davis,[1] Ben M. Garland,[1] Ryan Thorpe,[2] and Nicholas C. Strandwitz[1,a)]

AFFILIATIONS

[1]Department of Materials Science and Engineering, Lehigh University, Bethlehem, Pennsylvania 18015, USA
[2]Lehigh University Institute for Functional Materials and Devices, Bethlehem, Pennsylvania 18015, USA

Note: This paper is part of the Special Topic on Wide Bandgap Semiconductor Materials and Devices.
[a)]**Author to whom correspondence should be addressed:** nis212@lehigh.edu

ABSTRACT

Atomic layer deposited (ALD) niobium oxide (NbO_x) films were investigated for their passivation properties through minority carrier lifetime measurements and compared to a well-known passivating material, aluminum oxide. ALD alumina is known to passivate by a combination of field-effect passivation from fixed charges and chemical passivation from hydrogenation of dangling bonds. It was hypothesized that niobium oxide films passivate by varying degrees of the same mechanisms found in alumina. The effects of ALD oxygen source (water or ozone) and varying anneal temperatures were correlated to passivation quality. Lifetimes of sub-1 nanometer films were specifically investigated. It was found that water is a superior oxidant for passivation relative to O_3. Thermally activated NbO_x films deposited with water have near equivalent or superior lifetimes to alumina of the same thickness after equivalent annealing at temperatures up to 350 °C. Chemical analyses by x-ray photoelectron spectroscopy (XPS) were used to investigate the suspected mechanisms of passivation. It was suggested that field-effect passivation is the dominating mechanism in NbO_x films based on correlations between band movement as probed by XPS and the lifetime data presented in this work. This work provides new insights into the applicability of niobium oxide as a passivating selective contact for silicon photovoltaics with the goal of reaching new record efficiencies in solar cells.

INTRODUCTION

Solar photovoltaics are the fastest growing clean energy production technology.[1] High efficiency silicon solar cells can make a large contribution to reducing our overall carbon footprint with modern research-scale devices exceeding 25% light-to-energy conversion efficiency.[2] One technology contributing to these advances is passivating carrier-selective contacts, commonly referred to as passivating contacts, that use wide bandgap transition metal oxides (TMOs).[3,4] Passivation reduces interfacial recombination by mitigating trap states at the interface that can serve as recombination centers and/or by electrostatically repelling one carrier polarity to reduce the probability of recombination.[5] Carrier-selectivity provides asymmetric carrier conduction such that electrons or holes are selectively extracted at a given contact.[6] Wide bandgap TMOs are specifically useful because they minimize the parasitic absorption seen in silicon heterojunction designs that use amorphous silicon. Typical hydrogenated amorphous silicon (a-Si:H) passivation layers have been shown to allow only ~30% of light absorbed in the a-Si:H layer to be converted to useful energy.[7] TMOs, with bandgaps generally >3 eV, allow a larger portion of incident light to reach the silicon absorber layer than a:Si:H.[3,8] While these contacts may make improvements upon traditional silicon-based solar cells in terms of cost and/or efficiency, there is limited understanding of the mechanisms that allow for efficient carrier extraction and successful passivation with TMOs.

Passivation is a key component of solar cells to increase minority carrier lifetime and conversion efficiencies.[9] Unpassivated surfaces and interfaces result in large carrier recombination rates that reduce efficiency. Aluminum oxide, or alumina, (Al_2O_3) is one of the best-known passivating materials for silicon[10–13] and passivates by a combination of chemical and field-effect passivation.[14–16] Chemical passivation results from the approximately 2–4 at. % hydrogen present in atomic layer deposited (ALD) Al_2O_3 thin films which passivates dangling silicon surface atoms after annealing, eliminating trap states.[14] This effect can be quantified in an interface defect density on the order of 10^{11} eV^{-1} cm^{-2} as compared to

a defect density on the order of $10^{13}\,eV^{-1}\,cm^{-2}$ for silicon with only its native oxide (SiO_x).[17,18] Field-effect passivation utilizes a fixed charge on the order of $-5\times10^{12}\,q\,cm^{-2}$ at the alumina/silicon interface to induce band bending in the silicon, repelling one carrier polarity and creating a depletion or inversion layer near the surface, therefore reducing recombination rates.[17]

In the search for new passivation and selective contact materials and for new understanding of passivation mechanisms, niobium oxide (NbO_x) has recently been examined as an electron-selective and passivating contact.[19,20] Atomic layer deposited NbO_x films made with (tert-butylimido)-tris(diethylamino)-niobium (TBTDEN) and H_2O precursors annealed at 300 °C in forming gas (10%/90% H_2/N_2) have been shown to contain approximately the same atomic percentage of hydrogen as Al_2O_3 films, as well as similar fixed charge and induced band bending.[19] NbO_x on a chemical SiO_x layer results in excellent passivation with lifetimes on the order of 2 ms in the 1–5 nm regime, notably independent of the film thickness.[19,20]

While effective passivation with NbO_x has been demonstrated in films as thin as 1 nm, little is known about the ability of NbO_x to passivate silicon surfaces in the ultrathin, <1 nm regime. Successful passivation with sub-nanometer films may enable increases in efficiency when implemented in a tunneling passivating contact, assuming the passivating layer is fully closed and free of pinholes.[21–23] In this report, we examine the passivation of ultrathin ALD NbO_x layers along with a range of annealing temperatures. We also compare the impact of H_2O and O_3 oxygen precursors on carrier lifetime.

EXPERIMENTAL METHODS

Samples of double-side polished 525 μm thick float zone n-type silicon (WaferPro) with a base lifetime of >1000 μs ($\rho \geq 10\,000\,\Omega\,cm$) were diced and sonicated for 5 min in isopropyl alcohol and treated for 5 min per side in a UV-O_3 chamber (Jelight) before a 1 min soak in 5% hydrofluoric acid. Wafers were then cleaned by Radio Corporation of America (RCA) solutions 1 and 2, forming a thin layer of SiO_x (~1.5 nanometers).[24] Niobium oxide films with target thicknesses between 0.5 and 5 nm were deposited in a Savannah S-100 atomic layer deposition system at 150 °C with (tert-butylimido)-tris(diethylamino)-niobium (TBTDEN) and either H_2O or O_3 oxidants at an anticipated growth per cycle of approximately 0.54 or 0.41 Å/cycle, respectively, based on previous observation. Single sided test grade silicon samples were simultaneously processed for spectroscopic ellipsometry (SE) measurements to verify ALD film thickness. SE results were fit to a Cauchy model for a non-absorbing film with the SiO_x thickness separately accounted for based on a control sample. The NbO_x thicknesses correlated well with the number of ALD cycles, although some error may exist in the exact thicknesses. Samples were sequentially annealed in a 4-in. tube furnace between 200 and 450 °C for 60 min in a 5%/95% H_2/N_2 forming gas environment (flow rate ≈ 1.1 l/min) at ambient pressure with a furnace ramp rate of approximately 6 °C per minute.

Lifetime measurements were performed after each anneal with a Sinton WCT-120 in transient mode at a minority carrier density of $10^{15}\,cm^{-3}$ [with the exception of low lifetime control samples containing no niobium oxide, which were measured in Generalized (1/1) mode at $5\times10^{14}\,cm^{-3}$ minority carrier density]. Measurements were averaged over a series of five flashes and lifetimes reported are the average of two samples for each thickness. A matching experiment was done with ALD Al_2O_3 films grown with trimethylaluminum (TMA) and H_2O deposited on identical substrates, also at 150 °C with matching post-deposition annealing conditions, to compare the NbO_x passivation to a well-known passivating material (Fig. 1).

X-ray photoelectron spectroscopy (XPS) was performed to analyze film stoichiometry and to investigate band bending and gap states in samples with 2 and 10 nm niobium oxide films deposited with water. These samples were processed the same as above, but low resistivity n-type silicon wafers were used ($\rho = 0.053\,\Omega\,cm$). XPS was done in a custom-built SPECS instrument equipped with a DeviSim near-ambient pressure environmental chamber and *in situ* annealing capabilities. Heating was done via a 600 V electron beam heater directed at the backside of the sample holder and measured by a thermocouple clipped under the sample with sufficient time allowed at each temperature for the sample surface to stabilize. A monochromatic 1486.6 eV Al K_α x-ray source was used, and ejected electrons traveling normal to the sample plane were used for analysis. Spectra were fit to an approximately 20% Lorentzian and 80% Gaussian broadening, and all spectra were normalized to the C1s peak with energy 284.8 eV unless otherwise specified. Spectra were taken in the as-deposited state in ultrahigh vacuum, after *in situ* sequential anneals between 200 and 400 °C in a 5%/95% H_2/N_2 forming gas environment (P = 1 mbar) and again after the sample was cooled in ultrahigh vacuum. The backside of the sample was grounded to the XPS instrument, and no charge compensation was used.[25]

RESULTS AND DISCUSSION

Lifetime

Niobium oxide films deposited with both water and ozone showed increasing lifetimes with anneal temperature up to 350 °C

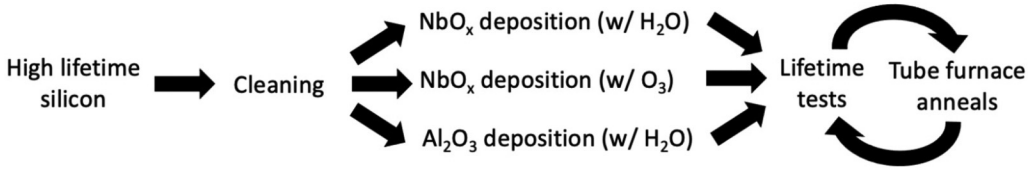

FIG. 1. Flow chart of wafer processing and lifetime testing.

(Fig. 2). The lifetime of the O_3 samples had a slight dependence on film thickness while the H_2O samples had little dependence on thickness (variation <0.3 ms) for samples greater than 1 nm in thickness and annealed above 200 °C. Sub-nanometer samples showed slightly lower lifetimes compared to the >1 nm samples but remained high relative to uncoated control samples. It is possible that these ultrathin ALD layers are not fully closed, leaving some of the surface passivated by only the native silicon oxide layer. However, it is clear from Fig. 2 that sub-1 nm films still largely improve upon the lifetime compared to samples with no NbO_x.

The lifetime data indicate a potential for the presence of both chemical and field-effect passivation in these films. The samples deposited with H_2O had longer lifetimes at all temperatures than those deposited with O_3, which may be due to the hydrogen in water increasing the potential for hydrogenation of dangling bonds and chemical passivation. Additionally, it has been established that fixed charges causing field-effect passivation often occur in the first 1–2 nm of passivating films.[14,17,26] Therefore, increases in film thickness beyond 1–2 nm would have no effect on the degree of field-effect passivation since the fixed charge would saturate in the first few nanometers. Xin *et al.* previously investigated changes in fixed charge in Al_2O_3 films and showed that at 425 °C, the magnitude of fixed charge saturates at approximately 11 cycles of Al_2O_3 (~1.4 nm).[17] The relative independence of lifetime from NbO_x thickness may be caused by the saturation of fixed charge at approximately 1 nm with additional film thickness having no significant effect on the lifetime. Furthermore, sub-nanometer films may suffer slightly lower lifetimes because there is insufficient film thickness for fixed charge saturation or retention of H.

To benchmark the NbO_x film performance as a passivation layers, we compared the results to those of identically processed Al_2O_3 layers [Figs. 2(c) and 3(b)]. Alumina samples showed similar behavior to NbOx films for thicknesses up to approximately 1.5 nm with monotonic increases in lifetime with sequential annealing steps. Notably, the thicker alumina films (t = ~2 and 5 nm) showed shorter lifetimes under these lower temperature annealing conditions. The trend observed for Al_2O_3 above 1.5 nm in Fig. 2(c) could not be explained, however, a similar relationship with thickness has been previously observed for uncapped alumina.[21] Al_2O_3 is typically annealed at ≥400 °C, at which temperature our samples still converge to the expected lifetime on the order of >4 ms in Fig. 3(b).[15,17,27] Thus, we believe our alumina control samples are similar to literature precedent for the relationship between thickness and annealing temperatures. NbO_x deposited with H_2O exhibited equivalent or superior passivation to Al_2O_3 at anneal temperatures up to 350 °C once thermally activated at 200 °C or above. The 5 nm NbO_x samples have a notably higher lifetime than the matching Al_2O_3 samples after anneals up to 350 °C. However, for higher anneal temperatures of 400 and 450 °C, the NbO_x lifetime decreases while the Al_2O_3 samples lifetime increases, most notably for the 5 nm sample (Fig. 3). This increase in lifetime is likely caused by an increase in the magnitude of negative fixed charge in the Al_2O_3 film at high temperatures.[15] The lifetimes at these higher anneal temperatures (> ~3.5 ms) are consistent with the typical lifetime-optimized temperatures reported in the literature.[3,17,28]

The decrease of the niobium oxide lifetime above 350 °C indicates changes in one or more passivating mechanisms that can be used to analyze the dominant mechanism acting in NbO_x. These changes are likely the result of a decrease in the degree of field-effect passivation from a reduced magnitude of fixed charge or a decrease in chemical passivation.

X-ray photoelectron spectroscopy

Stoichiometry

An x-ray photoelectron spectroscopy investigation with *in situ* anneals in forming gas in a custom-built near-ambient pressure analysis chamber was undertaken to examine the chemistry of the NbO_x film and to probe the fixed charge, and hence, field-effect passivation. The stoichiometry of the film was found by calculating the area of each core level peak and normalizing by its Scofield cross section and mean free path. The O:Nb atomic ratio of both the 2 and 10 nm films was found to be approximately 2.2–2.4. This ratio is consistent with substoichiometric Nb_2O_5 (O:Nb < 2.5), in agreement with the previous literature on ALD NbO_x films.[29] The components of the O1s peak attributed to O–Nb and O–Si bonds are well separated so it is unlikely that oxygen present within the SiO_x layer affected the calculated O:Nb ratios.

Deconvolution of the Nb3d peaks could not be done unambiguously so the specific niobium oxidation states were not determined. However, *in situ* XPS analysis showed a clear increase in peak binding energies with temperature on the order of 0.9 eV between the as-deposited state and 400 °C when normalized to C1s (Fig. 4). Movement in binding energies can occur from changes in

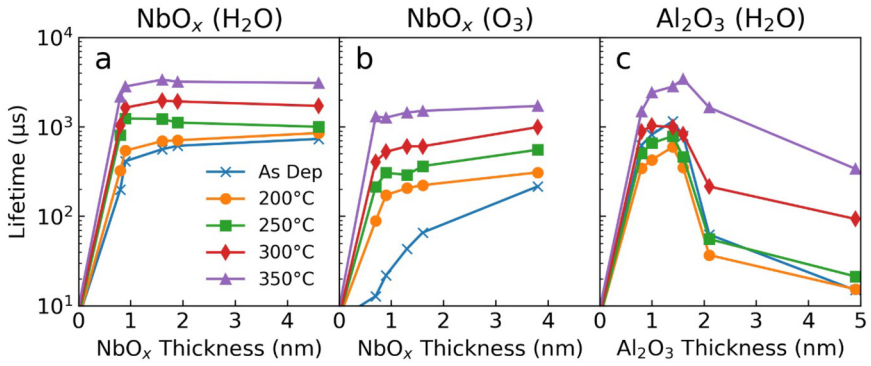

FIG. 2. Minority carrier lifetime for as-deposited and annealed films of (a) NbO_x deposited with H_2O, (b) NbO_x deposited with O_3, and (c) Al_2O_3 deposited with H_2O.

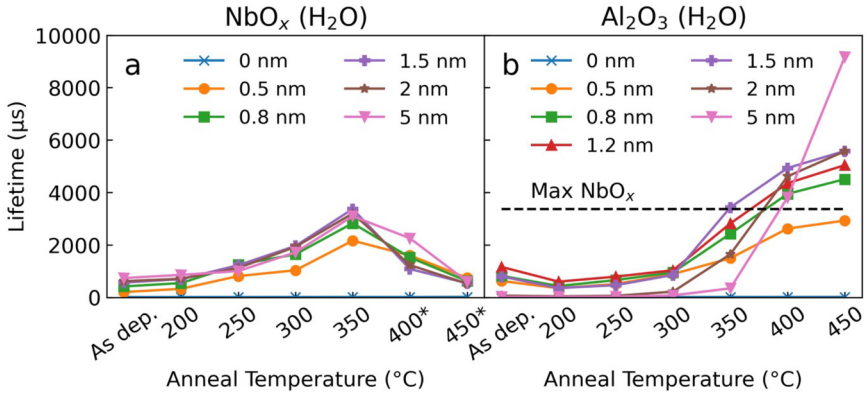

FIG. 3. Minority carrier lifetime as a function of temperature for (a) NbO_x deposited with H_2O and (b) Al_2O_3 deposited with H_2O (*400 and 450 °C anneals done approximately 2 months after sample fabrication).

the bonding state of the niobium atoms or from electrostatic effects in the film. To determine which mechanism is present here, the Nb3d binding energy was also normalized to O1s. Separate normalizations to both C1s and O1s are shown in Fig. 4 and it is clear that the O1s and Nb3d binding energies shift together relative to C1s. This collective shift indicates that the movement is likely not caused by changes in the Nb–O bonding. Typically, it would be expected that in the case of electrostatic changes the C1s peak would shift along with the Nb3d and O1s, accompanied by bending of the Si bands. However, since the carbon is mostly on the surface of the film, it is possible that the forming gas passing over the surface of the sample in the environmental cell of the instrument may allow for discharge of the surface carbons but not the NbO_x. An electrostatic-based increase in binding energy with increasing temperature would be consistent with a decrease in magnitude of a previously existing negative charge in the NbO_x film.[19] Negative charges in Al_2O_3 films have previously been attributed to aluminum vacancies and/or oxygen interstitials, resulting in an oxygen rich region of the film near the interface.[14,26] The proposed decrease in negative fixed charge density in NbO_x may be caused by a reduction in the number of V_{Nb} and O_i; however, the degree of intrinsic defects that would result in a fixed charge would not be quantifiable by XPS analysis. Alternatively, negative fixed charges resulting from acceptor-type doping of the SiO_x layer by transition metals drawn from TMO layers have been observed in Al_2O_3 and HfO_2 films.[30] Removal of Nb doping from the SiO_x layer at higher temperatures may also cause a decrease in negative fixed charge; however, it is unlikely that the anneal temperatures in this experiment are sufficient for these bonding changes to occur.

Band bending

Movements of the Si2s and Si2p core peaks were used to investigate changes in band bending near the interface as XPS has previously been used to successfully probe band bending at silicon interfaces.[25,31] No charge compensation or normalization was done

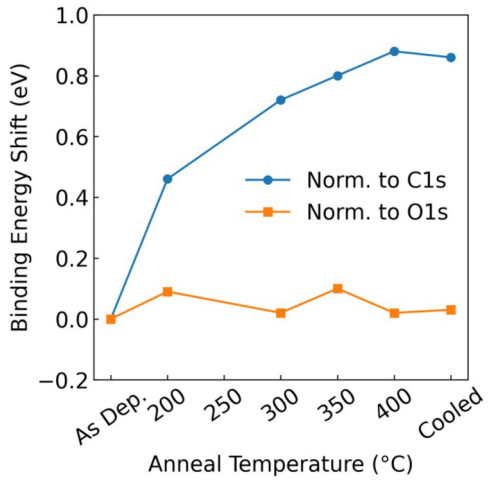

FIG. 4. Change in binding energy of Nb3d peak with thermal processing when normalized to C1s and O1s.

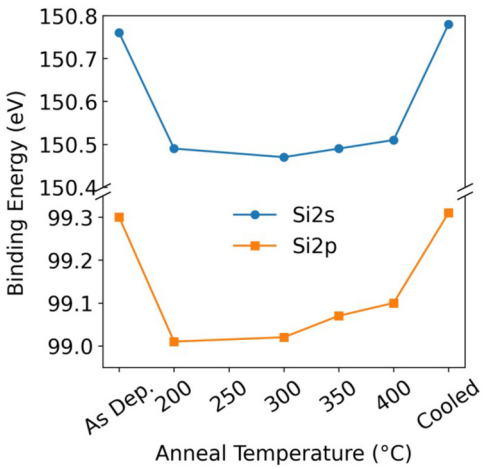

FIG. 5. Si2s and Si2p binding energies as a function of anneal condition.

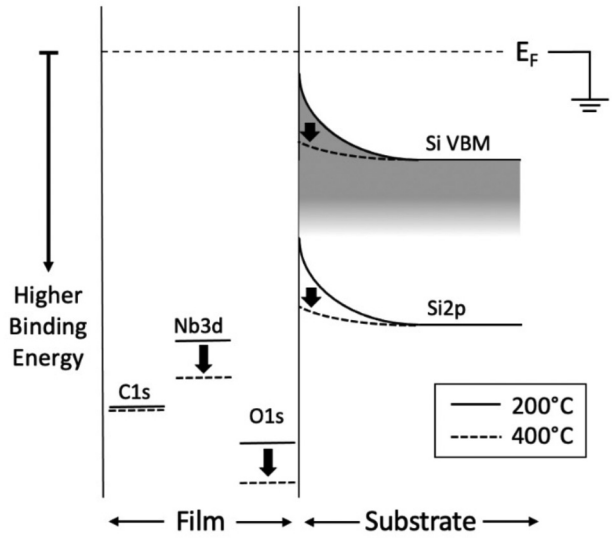

FIG. 6. Schematic showing a constant C1s energy level while the Nb3d and O1s shift together to increased binding energy and the Si2p band bending at the interface decreases, decreasing the degree of field-effect passivation between 200 and 400 °C (not to scale).

to allow the silicon bands to move freely. Both the Si2s and Si2p spectra showed high binding energies in the as-deposited and cooled cases (possibly a charging effect) and relatively no change between 200 and 300 °C. However, both showed an increase in binding energy on the order of 100 meV between 300 and 400 °C, which would be on the order expected for changes in band bending[32] and would correspond to the valence band maximum moving further away from the Fermi level (Fig. 5). This movement is consistent with the electrostatic changes suspected in the film since a decrease in magnitude of a pre-existing negative charge would allow the initially upward bent silicon bands to relax as more electrons reach the interface, reducing the degree of field-effect passivation present between 300 and 400 °C (Fig. 6). This temperature range also corresponds to the decrease in lifetime seen above 350 °C in Fig. 2, and this correlation suggests that a degree of field-effect passivation may be present in annealed NbO_x films. Previous surface photovoltage (SPV) measurements have also shown an induced band bending of ~840 meV, consistent with previously observed band bending in alumina passivated n-Si.[19]

Gap states

The valence band spectra of the 10 nm NbO_x film sample was measured to examine gap states between the Fermi edge at 0 eV and the valence band minimum of the niobium oxide film. States were observed between 1 and 2 eV in binding energy [Fig. 7(a)]. The presence of some intensity from the silicon valence band could not be ruled out; however, this contribution was not expected to change with temperature, so relative changes in the valence band intensity at a given energy may be attributed to changes in the gap states in the NbO_x.

Changes in intensity of the photoelectron spectra with temperature at 1.6 eV indicate the number of gap states increases linearly with temperature up to 400 °C before decreasing back to approximately the 300 °C level upon cooling [Fig. 7(b)]. This suggests an increase in trap state density as temperature increases which may contribute to a decrease in chemical passivation, possibly due to increases in O vacancies. However, the lifetime was shown to increase up to 350 °C despite the increase in gap states suggesting that field-effect passivation dominates in NbO_x.

Stability

After the 350 °C anneal, the NbO_x samples grown using H_2O were left in the dark in lab air for approximately 1 month to investigate their passivation stability. Following this ageing, the average lifetime decreased to approximately the 200 °C anneal level (Fig. 8). Interestingly, re-annealing these samples at the same maximum temperature of 350 °C returned the lifetime approximately back to the lifetime of the original 350 °C anneal. This may indicate that if field-effect passivation is present, some of the assumed fixed charges are actually temporary or trapped charges. These data are superimposed on the 200 and 350 °C samples from Fig. 2(a) in

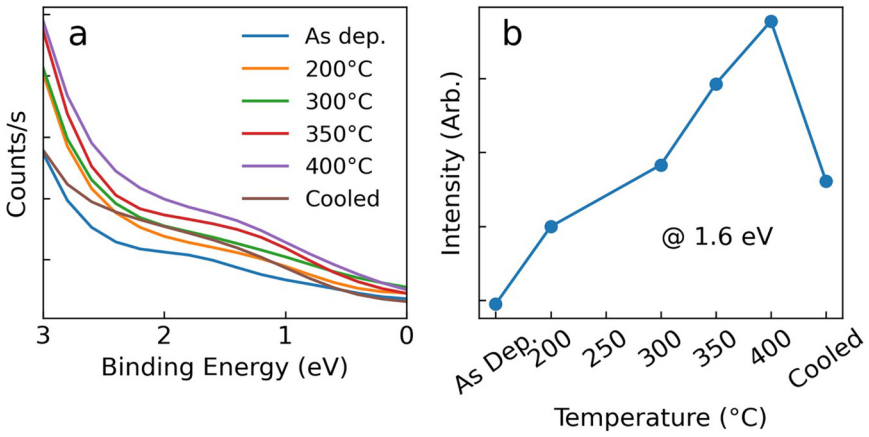

FIG. 7. Intensity of smoothed and normalized valence band spectra at 1.6 eV binding energy indicating and increase in gap states with anneal temperature.

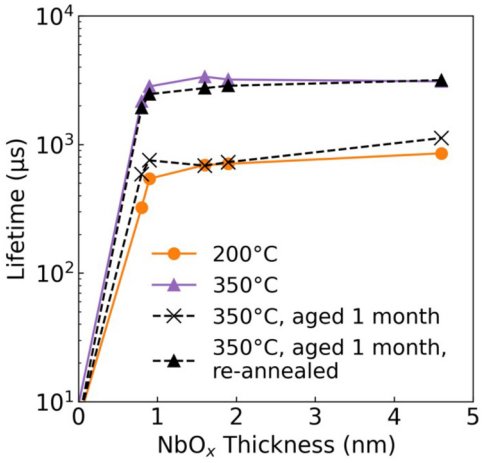

FIG. 8. Stability of lifetime after 1 month and after re-anneal at 350 °C.

Fig. 8. These results can be related to previous work by Macco *et al.* in which light-soaking was shown to improve lifetimes of samples with ALD NbO_x films through injection of negative charges serving to improve field-effect passivation.[19] Here, the decrease in lifetime after an extended period in the dark followed by a resurrection of the original lifetime may relate to a re-injection of negative charges, returning a field-effect passivation component to its original state.

CONCLUSION

The passivation of atomic layer deposited niobium oxide thin films deposited on silicon with water and ozone oxidants was investigated for application as a passivating layer in wide bandgap transition metal oxide carrier-selective contacts. It was determined that H_2O is the superior oxidant for passivation with a peak lifetime of 3.4 ms achieved for a 1.6 nm sample annealed at 350 °C. Lifetimes in samples deposited with H_2O were relatively independent of thickness above 1 nm and were near equivalent or superior to ALD aluminum oxide lifetimes up to an annealing temperature of 350 °C with the exception of the as-deposited state. NbO_x sample lifetimes decreased; however, when annealed at 400 and 450 °C, while Al_2O_3 sample lifetimes improved at these temperatures. Sub-nanometer thicknesses maintained high lifetimes but were consistently slightly lower than the lifetimes in samples with >1 nm films.

The stoichiometry of the NbO_x films was determined to be substoichiometric Nb_2O_5 via quantitative x-ray photoelectron spectroscopy analysis. Additionally, the binding energy of the O1s and Nb3d peaks were seen to increase with temperature which was attributed to a possible decrease in negative charge in the film. Movement of the silicon core peaks on the order of 100 meV was also attributed to downward movement of the silicon bands near the interface. Based on the known presence of negative fixed charge in NbO_x films,[19] it was suggested that a decrease in the magnitude of negative charge density of the film occurred with temperature and the initially upward bent silicon bands were allowed to relax, decreasing the degree of field-effect passivation present. The correlation between this band movement as probed by XPS and the reduction of lifetime above 350 °C supports the hypothesis that field-effect passivation is the dominating mechanism in ALD NbO_x films.

There is potential for an increase in passivation by NbO_x films if both chemical and field-effect passivation can be independently quantified and improved. This may aid in increasing lifetimes above 350 °C and make NbO_x more competitive with Al_2O_3 as a passivating layer. Additional work also needs to be done on the carrier-selective potential of niobium oxide films and to optimize films for effective combined passivation and carrier-selectivity.

ACKNOWLEDGMENTS

The authors gratefully acknowledged funding from the U.S. National Science Foundation (No. CBET-1605129).

AUTHOR DECLARATIONS

Conflict of Interest

The authors declare on conflicts of interest.

DATA AVAILABILITY

The data that support the findings of this study are available from the corresponding author upon reasonable request.

REFERENCES

[1]See https://www.seia.org/solar-industry-research-data for "Solar Industry Research Data | SEIA."
[2]K. Yoshikawa *et al.*, "Silicon heterojunction solar cell with interdigitated back contacts for a photoconversion efficiency over 26%," Nat. Energy **2**, 17032 (2017).
[3]J. Melskens *et al.*, "Passivating contacts for crystalline silicon solar cells: From concepts and materials to prospects," IEEE J. Photovolt. **8**, 373–388 (2018).
[4]T. G. Allen, J. Bullock, X. Yang, A. Javey, and S. De Wolf, "Passivating contacts for crystalline silicon solar cells," Nat. Energy **4**(4), 914–928 (2019).
[5]L. E. Black *et al.*, "Explorative studies of novel silicon surface passivation materials: Considerations and lessons learned," Sol. Energy Mater. Sol. Cells **188**, 182–189 (2018).
[6]U. Wurfel, A. Cuevas, and P. Wurfel, "Charge carrier separation in solar cells," IEEE J. Photovolt. **5**, 461–469 (2015).
[7]Z. C. Holman *et al.*, "Current losses at the front of silicon heterojunction solar cells," IEEE J. Photovolt. **2**, 7–15 (2012).
[8]X. Yang, K. Weber, Z. Hameiri, and S. De Wolf, "Industrially feasible, dopant-free, carrier-selective contacts for high-efficiency silicon solar cells," Prog. Photovolt. Res. Appl. **25**, 896–904 (2017).
[9]P. Gao *et al.*, "Dopant-free and carrier-selective heterocontacts for silicon solar cells: Recent advances and perspectives," Adv. Sci. **5**, 1700547 (2018).
[10]S. Li *et al.*, "Excellent silicon surface passivation using dimethylaluminium chloride as Al source for atomic layer deposited Al_2O_3," Phys. Status Solidi A **212**, 1795–1799 (2015).
[11]S. Bordihn *et al.*, "High surface passivation quality and thermal stability of ALD Al_2O_3 on wet chemical grown ultra-thin SiO_2 on silicon," Energy Procedia **8**, 654–659 (2011).
[12]N. Batra *et al.*, "Influence of deposition temperature of thermal ALD deposited Al_2O_3 films on silicon surface passivation," AIP Adv. **5**, 067113 (2015).

[13]J. Schmidt *et al.*, "Fuzzy discrete event systems for multiobjective control: Framework and application to mobile robot navigation," IEEE Trans. Fuzzy Syst. **20**, 910–922 (2012).
[14]G. Dingemans and W. M. M. Kessels, "Status and prospects of Al_2O_3-based surface passivation schemes for silicon solar cells," J. Vac. Sci. Technol. A **30**, 040802 (2012).
[15]S. Kühnhold-Pospischil, P. Saint-Cast, A. Richter, and M. Hofmann, "Activation energy of negative fixed charges in thermal ALD Al_2O_3," Appl. Phys. Lett **109**, 061602 (2016).
[16]S. Banerjee and K. Mukul Das, "A review of Al_2O_3 as surface passivation material with relevant process technologies on c-Si solar cell," Opt. Quantum Electron. **53**, 60 (2021).
[17]Z. Xin *et al.*, "Surface passivation investigation on ultra-thin atomic layer deposited aluminum oxide layers for their potential application to form tunnel layer passivated contacts related content," Jpn. J. Appl. Phys. **56**, 08MB14 (2017).
[18]E. H. Poindexter *et al.*, "Electronic traps and Pb centers at the Si/SiO_2 interface: Band-gap energy distribution," J. Appl. Phys. **56**, 2844 (1984).
[19]B. Macco *et al.*, "Effective passivation of silicon surfaces by ultrathin atomic-layer deposited niobium oxide," Appl. Phys. Lett. **112**, 242105 (2018).
[20]B. Macco *et al.*, "Atomic-layer deposited Nb_2O_5 as transparent passivating electron contact for c-Si solar cells," Sol. Energy Mater. Sol. Cells **184**, 98–104 (2018).
[21]B. E. Davis and N. C. Strandwitz, "Aluminum oxide passivating tunneling interlayers for molybdenum oxide hole-selective contacts," IEEE J. Photovolt. **10**, 722–728 (2020).
[22]T. F. Wietler *et al.*, "Pinhole density and contact resistivity of carrier selective junctions with polycrystalline silicon on oxide," Appl. Phys. Lett. **110**, 253902 (2017).
[23]R. Peibst *et al.*, "Working principle of carrier selective poly-Si/c-Si junctions: Is tunnelling the whole story?," Sol. Energy Mater. Sol. Cells **158**, 60–67 (2016).
[24]W. Kern, "The evolution of silicon wafer cleaning technology," J. Electrochem. Soc. **137**, 1887–1892 (1990).
[25]D. C. Gleason-Rohrer, B. S. Brunschwig, and N. S. Lewis, "Measurement of the band bending and surface dipole at chemically functionalized Si(111)/vacuum interfaces," J. Phys. Chem. C **117**(35), 18031–18042 (2013).
[26]B. Shin *et al.*, "Origin and passivation of fixed charge in atomic layer deposited aluminum oxide gate insulators on chemically treated InGaAs substrates," Appl. Phys. Lett. **96**, 152908 (2010).
[27]A. Richter, J. Benick, M. Hermle, and S. W. Glunz, "Reaction kinetics during the thermal activation of the silicon surface passivation with atomic layer deposited Al_2O_3," Appl. Phys. Lett **104**, 061606 (2014).
[28]G. Kaur *et al.*, "Can interface charge enhance selectivity in tunnel layer passivated contacts? Using negatively charged aluminium oxide capped with dopant free PEDOT or boron doped polysilicon," Sol. Energy Mater. Sol. Cells **221**, 110857 (2021).
[29]S. B. Basuvalingam *et al.*, "Comparison of thermal and plasma-enhanced atomic layer deposition of niobium oxide thin films," J. Vac. Sci. Technol. A **36**, 041503 (2018).
[30]J.-P. Lehtiö *et al.*, "Observation of Si 2p core-level shift in Si/high-κ dielectric interfaces containing a negative charge," Adv. Electron. Mater **7**, 2100034 (2021).
[31]M. Ç. Opuroğ Lu, H. Sezen, R. L. Opila, and S. Suzer, "Band-bending at buried SiO_2/Si interface as probed by XPS," ACS Appl. Mater. Interfaces **5**(12), 5875–5881 (2013).
[32]B. E. Coss *et al.*, "Measurement of Schottky barrier height tuning using dielectric dipole insertion method at metal-semiconductor interfaces by photoelectron spectroscopy and electrical characterization techniques," J. Vac. Sci. Technol. B **31**, 021202 (2013).